Check for updates

LIMNOLOGY and OCEANOGRAPHY

ASLO

Limnol. Oceanogr. 9999, 2024, 1–14
© 2024 The Author(s). *Limnology and Oceanography* published by Wiley Periodicals LLC on behalf of Association for the Sciences of Limnology and Oceanography.
doi: 10.1002/lno.12671

Nutrient availability influences the thermal response of marine diatoms

Mengwen Pang[1] **Kailin Liu**[2] **Bingzhang Chen**[3] **Xiaodong Zhang**[1] **Zuyuan Gao**[1] **Zhimeng Xu**[1] **Yehui Tan**[4] **Jing Yang**[1] **Hongbin Liu**[1,5*]

[1]Department of Ocean Science, Hong Kong University of Science and Technology, Hong Kong, China
[2]College of the Environmental and Ecology, Xiamen University, Xiamen, China
[3]Department of Mathematics and Statistics, University of Strathclyde, Glasgow, UK
[4]Key Laboratory of Tropical Marine Bio-resources and Ecology, South China Sea Institute of Oceanology, Chinese Academy of Science, Guangzhou, China
[5]Southern Marine Science and Engineering Guangdong Laboratory (Guangzhou), Guangzhou, China

Abstract

Understanding how phytoplankton growth responds to temperature is critical for forecasting marine productivity in a warming ocean. While previous laboratory studies have shown that phytoplankton thermal traits such as optimal temperature (T_{opt}) can be affected by nutrient availability, it is unclear whether this can be extrapolated to natural communities. To address this, we tested the impacts of nutrient availability on the thermal responses of two cosmopolitan diatom genera, *Pseudo-nitzschia* and *Leptocylindrus*, through a series of in situ manipulation experiments on natural phytoplankton communities. Analysis of the thermal performance curves revealed that nutrient limitation during summer not only limited the growth of these two genera but also reduced their T_{opt} and the maximum growth rates (μ_{max}). T_{opt} was close to or lower than in situ temperature under ambient nutrient conditions, suggesting that further warming may have a detrimental effect on their growth. However, increasing nutrient supply could counteract this by enhancing T_{opt} and μ_{max}. To further confirm the interactive effects of nutrients and temperature on diatoms, we analyzed a 20-yr monitoring dataset on *Pseudo-nitzschia*, *Leptocylindrus*, and the whole diatom assembly in Hong Kong coastal waters. We found that the abundances of marine diatoms were significantly higher at high temperatures under nutrient-rich environments while relatively low under low nutrient concentrations. Findings on natural diatom cell density align with the growth performance derived from in situ manipulation experiments, suggesting that abundant nutrients bolster marine diatoms in coping with warming. Our results highlight the importance of considering the influence of nutrient availability on thermal response of phytoplankton growth, which sheds light on how marine primary production may change under climate warming.

Marine phytoplankton in the sunlit upper ocean contribute about 50% of global primary production with 1% photosynthetic biomass (Field et al. 1998). By capturing carbon dioxide and converting it into organic matter, phytoplankton play a vital role in global biogeochemical cycles and climate regulation (Falkowski 2012; Fussmann et al. 2014), which are affected by temperature and nutrient availability (Sarmiento et al. 2004; Elser et al. 2007).

Temperature-dependent phytoplankton growth is crucial for determining marine primary production (Sarmiento et al. 2004), which is usually described by the thermal performance curve showing a unimodal and left-skewed pattern within a sufficiently wide temperature range. Previous studies on phytoplankton growth focused mostly on the "physiological temperature range," that is, the temperature range below the optimal temperature (T_{opt}) of growth (Pawar et al. 2016; Liu et al. 2019). In these studies, temperature sensitivity, in terms of Q_{10} in Eppley curve (Eppley 1972) or activation energy in Boltzmann–Arrhenius model (BA model; Brown et al. 2004), defining how fast metabolic rates increase with temperature before reaching T_{opt}, was often used to forecast phytoplankton growth and planktonic food web structure in

*Correspondence: liuhb@ust.hk

Additional Supporting Information may be found in the online version of this article.

This is an open access article under the terms of the Creative Commons Attribution-NonCommercial License, which permits use, distribution and reproduction in any medium, provided the original work is properly cited and is not used for commercial purposes.

Author Contribution Statement: HL, MP, and KL conceived and designed the study. Sample collection and measurements were performed by MP, KL, ZG, ZX, and YY. MP, XZ, ZG, and JY helped to compile the historical dataset. MP analyzed data and drafted the manuscript. MP, KL, BC, and HL interpreted the data and revised the manuscript. All authors approved the final manuscript.
Mengwen Pang and Kailin Liu should be considered the joint first authors.

future ocean (Chen et al. 2012; Chen and Laws 2017; Liu et al. 2019). However, the temperature sensitivity solely might be inadequate to quantify the thermal response of phytoplankton growth in the warming oceans as the current or future environmental temperature regime may exceed their T_{opt}, especially in (sub)tropical regions (Thomas et al. 2012; Liu et al. 2019). Therefore, evaluating other thermal traits, including T_{opt} and maximum growth rate (μ_{max}), and unraveling how they vary with the environmental factors is imperative in the context of ocean warming.

In addition to the effects of temperature, phytoplankton growth in nature can also be limited by resource availability, such as light and nutrients. Nutrient availability is a primary factor influencing phytoplankton growth (Marañón et al. 2015; Lehtinen et al. 2017), which is often the limiting factor in the ocean (Moore et al. 2013). Some studies have found that nutrient availability overrides temperature as a controlling factor of natural phytoplankton growth (O'Connor et al. 2009; Marañón et al. 2014). Global warming will strengthen ocean stratification and restrict nutrient supply from deeper waters, which would intensify both the area and severity of nutrient limitation in oligotrophic waters (Polovina et al. 2008; Irwin and Oliver 2009; Collins et al. 2013). Given that it is important to consider the nutrient effects when investigating temperature-dependent phytoplankton growth in natural environments.

However, many previous studies, particularly those Earth System Models that we rely on to predict the future state of the ocean, treat nutrient and temperature effects on phytoplankton growth separately and assume the thermal performance of phytoplankton growth as being independent of nutrients. Several pioneering studies have indicated that this is not the case (Thomas et al. 2017; Bestion et al. 2018; Liu et al. 2021). Liu et al. (2021) found that the temperature sensitivity of natural *Synechococcus* growth rate under in situ nutrient-limiting conditions was lower than under nutrient-replete conditions, which provides good insights into how nutrient availability affects the thermal response within the physiological temperature range. A recent laboratory and modeling study found that nitrogen limitation resulted in a decrease of 6°C for the T_{opt} of *Thalassiosira pseudonana*, suggesting that this diatom species is vulnerable to warm and nutrient-limited environments (Thomas et al. 2017). Nevertheless, few studies have estimated the T_{opt} of natural phytoplankton populations under various nutrient conditions. It is urgent to fill this research gap in whether and how nutrient availability influences T_{opt} of phytoplankton growth in situ.

To address it, we investigated the nutrient dependency of thermal responses of diatoms in the subtropical coastal regions of the South China Sea (Fig. 1). Diatoms, as one important primary producer in the ocean, contribute around 20% of global primary production, especially in coastal and upwelling regions (Nelson et al. 1995; Falkowski 2012; Malviya et al. 2016). We conducted a series of in situ temperature–nutrient modulation experiments focusing on two diatom genera, *Pseudo-nitzschia* and *Leptocylindrus*, and analyzed the data based on the genus level. These two genera are identified as the top 10 most abundant diatom genera in the global ocean (Malviya et al. 2016; Tréguer et al. 2018). They are common in our study area and even dominate the whole diatom community sometimes (Supporting Information Figs. S1, S2). In addition to the manipulation experiments, we also analyzed a 20-yr monthly monitoring dataset in Hong Kong coastal waters to test whether our findings from in situ manipulation experiments are consistent with long-term dynamics of *Pseudo-nitzschia* and *Leptocylindrus* and if they can apply to the whole diatom assemblage.

Materials and methods

Study area and experimental setup

We conducted a series of temperature–nutrient–manipulated experiments at five subtropical coastal stations, that is, EP03, P03, PM6, PM7, and PM8 (Fig. 1). Stats. EP03 and P03, located at the mouth of the Pearl River Estuary (PRE), are more nutrient-enriched because of the river discharges and anthropogenic activities. Stas. PM6, PM7, and PM8 are on the eastern side of Hong Kong waters, barely influenced by the Pearl River but affected by the China Coastal Current and oceanic water from the South China Sea. We collected surface seawater (0.5–1 m in depth with the ambient irradiance around 150–200 μmol photons m^{-2} s^{-1}) using Niskin bottles attached to a CTD (Sea Bird Electronics, Inc.) at Stas. EP03 and P03 in July 2021 and acid-washed Nalgene Polycarbonate Carboys (Thermo Fisher) at Stas. PM6, PM7, and PM8 in August 2021. The in situ water temperature was measured with a CTD sensor at Stas. EP03 and P03 and a YSI EXO2 multiprobe sensor at Stas. PM6, PM7, and PM8.

For the nutrient setting, in addition to the in situ nutrient condition at the five experimental stations, nutrient amendments were conducted at each station. A gradient of dissolved inorganic nitrogen (DIN, i.e., $NO_3^+ + NH_4^+$, 9 : 1 in ratio) along with PO_4^{3-}, SiO_3^{2-}, Fe^{3+}, and Mn^{2+} in a fixed ratio (i.e., Redfield ratio) was added to the incubation bottles (Table 1; Supporting Information Table S1). For Stas. EP03 and P03, considering their relatively high in situ nutrient concentration, only one nutrient-amended level (i.e., nutrient-depleted condition; Table 1) was conducted to ensure sufficient nutrient supply for diatom growth. Whereas at Stas. PM6, PM7, and PM8, given their low in situ nutrient concentrations, four or five nutrient-amended levels were settled at each station to access more nutrient conditions (Table 1).

To investigate thermal responses under each nutrient condition, bottles with different nutrient additions were incubated at five temperatures: in situ temperature (T), $T - 5$°C, $T - 3$°C, $T + 3$°C, and $T + 5$°C (Table 1; samples at $T - 5$°C at Sta. PM7 were lost due to instrument malfunction) for 1 d. The temperatures were prudently designed considering the potential impacts of temperature extremes on organisms during the short-term incubation experiments, commonly referred to as "thermal shock" (Liu et al. 2019, 2021).

19395590, 0, Downloaded from https://aslopubs.onlinelibrary.wiley.com/doi/10.1002/lno.12671 by University Of Strathclyde, Wiley Online Library on [02/09/2024]. See the Terms and Conditions (https://onlinelibrary.wiley.com/terms-and-conditions) on Wiley Online Library for rules of use; OA articles are governed by the applicable Creative Commons License

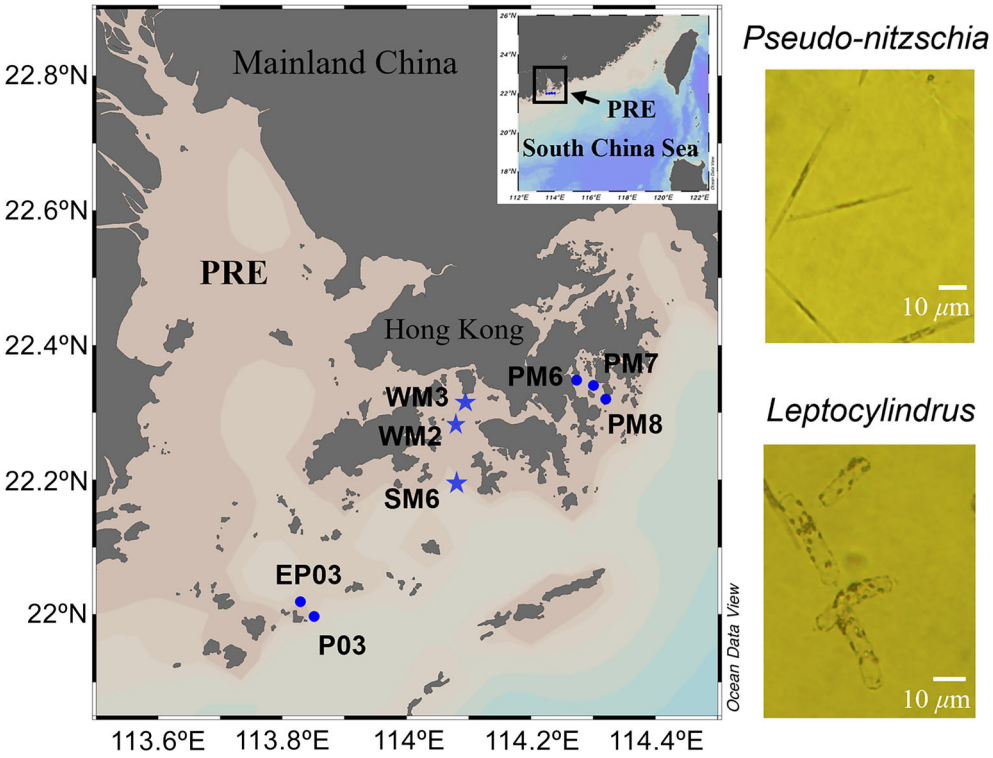

Fig. 1. Station locations and the targeted diatoms, *Pseudo-nitzschia* and *Leptocylindrus*. Dots represent temperature and nutrient manipulation experimental stations; stars represent long-term monitoring stations.

Diatom growth rates estimation under the aforementioned nutrient–temperature experimental conditions were based on the "two-point" dilution experiments modified from Landry and Hassett (1982), which has been verified as accurate as the traditional dilution approach with a full dilution gradient (Chen 2015; Morison and Menden-Deuer 2017). The dilution levels were set as 10% and 100% of natural seawater, respectively, based on previous findings by Chen (2015) and Morison and Menden-Deuer (2017). To achieve the 10% dilution level, we first prepared 2.16 liters of particle-free seawater by filtering the seawater through a 0.22-μm pore-size filter capsule (Pall Corporation) and added them to 2.4-liter polycarbonate bottles. Then, these bottles were subsequently filled with natural seawater prescreened through 200-μm mesh. As 10% is a highly diluted level, the grazing pressure on phytoplankton growth rates in the 10% bottles was very low and has been verified and treated as negligible by previous studies (Chen 2015; Morison and Menden-Deuer 2017; Anderson et al. 2022). As such, diatom net growth rates in 10% bottles were estimated as their instantaneous growth rate. For Stas. PM6, PM7, and PM6, we set the 10% dilution level for all nutrient levels, including the in situ nutrient condition (Table 1). Specifically, once the 10% dilution bottles were settled, we added the corresponding nutrients into the bottles and then put the bottles into corresponding temperature-control incubators. For Stas. EP03 and P03, the 10% dilution level was set for nutrient-amended conditions, whereas the 100% dilution level achieved by filling with prescreened seawater in the 2.4-liter polycarbonate bottles was set for both nutrient-amended and -unamended conditions. In that case, diatom growth rates under nutrient-unamended conditions were estimated according to the relationship between diatom net growth rates, diatom instantaneous growth rates, and microzooplankton grazing rates, with the specific calculation approach following Landry et al. (2011) and provided later. Duplicates (i.e., two bottles) were settled for each experimental treatment.

The manipulation of dilution and nutrients at each station was settled within 1.5 h once the in situ water was sampled. After that, all the bottles were incubated in the corresponding temperature-control incubators for 1 d to simulate the response of in situ diatom populations to environmental changes while avoiding the long-term closed-system–induced limitation of population capacity and resource exhaustion. The temperature of each incubator was controlled by the heater and chillers (RESUN, China) with internally circulated water. Temperature detectors (TH10R, MIAOXIN, China) were attached to the incubator to monitor the real-time water temperature, which was treated as the true experimental temperatures in later analysis. Neutral-density mesh was used to cover the incubators to mimic light conditions in the sampling depth, around 150–200 μmol photons m^{-2} s^{-1} detected by a light meter QSL-101 (Biospherical Instruments Inc.). All bottles, carboys, filters, and

19395590, 0, Downloaded from https://aslopubs.onlinelibrary.wiley.com/doi/10.1002/lno.12671 by University Of Strathclyde, Wiley Online Library on [02/09/2024]. See the Terms and Conditions (https://onlinelibrary.wiley.com/terms-and-conditions) on Wiley Online Library for rules of use; OA articles are governed by the applicable Creative Commons License

Table 1. Summary of the in situ environmental parameters at the beginning of experiments, nutrient–temperature manipulation settings, and the dilution levels at five manipulation experimental stations. Except for the in situ temperature (*T*), environmental parameters are shown by the mean value from triplicate. Nutrient conditions (N. con.) with their corresponding added concentrations in terms of DIN are provided. n_0 represents in situ nutrient condition (nutrient unamended) at each station; n_n represents nutrient-amended condition at Stas. EP03 and P03; n_1, n_2, n_3, n_4, and n_5 represent nutrient-amended conditions at Stas. PM6, PM7, and PM8, with different numbers indicating different levels of enrichments. Temperature setting under each nutrient condition is presented, with *T* representing the in situ environmental temperature at the corresponding stations. Dilution levels under each nutrient and temperature conditions are presented, with 100/10 representing both 100% and 10% dilution levels settled under this experimental condition. "—" represents no samples here.

	In situ environmental parameters							Nutrient manipulation		Temperature setting and dilution levels (%)				
Sta.	*T* (°C)	Chl *a* (μg L^{-1})	DIN (μM)	DIP (μM)	SiO_3^{2-} (μM)	*Pseudo-nitzschia* (cells mL^{-1})	*Leptocylindrus* (cells mL^{-1})	N. con.	Added DIN (μM)	*T* (°C)	*T* + 3°C	*T* + 5°C	*T* − 3°C	*T* − 5°C
P03	28.9	2.260	4.243	0.282	0.392	600	719	n_0	+0	100	100	100	100	100
								n_n	+20	100/10	100/10	100/10	100/10	100/10
EP03	29.5	3.343	13.793	0.586	1.729	1031	1058	n_0	+0	100	100	100	100	100
								n_n	+17.5	100/10	100/10	100/10	100/10	100/10
PM7	27.7	0.271	1.709	0.390	2.106	63	381	n_0	+0	10	10	10	10	—
								n_1	+1	10	10	10	10	—
								n_2	+4	10	10	10	10	—
								n_3	+10	10	10	10	10	—
								n_4	+30	10	10	10	10	—
PM6	29.6	0.168	1.428	0.353	3.176	61	451	n_0	+0	10	10	10	10	10
								n_1	+0.5	10	10	10	10	10
								n_2	+1	10	10	10	10	10
								n_3	+4	10	10	10	10	10
								n_4	+10	10	10	10	10	10
								n_5	+30	10	10	10	10	10
PM8	28.1	0.611	2.143	0.371	2.641	55	542	n_0	+0	10	10	10	10	10
								n_1	+0.5	10	10	10	10	10
								n_2	+1	10	10	10	10	10
								n_3	+4	10	10	10	10	10
								n_4	+10	10	10	10	10	10
								n_5	+30	10	10	10	10	10

19395590, 0, Downloaded from https://aslopubs.onlinelibrary.wiley.com/doi/10.1002/lno.12671 by University Of Strathclyde, Wiley Online Library on [02/09/2024]. See the Terms and Conditions (https://onlinelibrary.wiley.com/terms-and-conditions) on Wiley Online Library for rules of use; OA articles are governed by the applicable Creative Commons License

silicon tubing used in our study were washed with 10% HCl, deionized water, MilliQ water, and in situ seawater before each experiment.

Diatom abundance and other parameter measurements at the manipulation stations

Samples for measuring in situ dissolved inorganic nutrients, that is, NO_2^-, NO_3^-, NH_4^+, PO_4^{3-}, and SiO_3^{2-}, were taken in triplicate by filtering the seawater through a 0.2-μm filter, stored in −20°C freezer, and analyzed by the Skalar auto-analyzer (San Plus system) according to the JGOFS protocol (Knap et al. 1994). To measure in situ chlorophyll *a* (Chl *a*) concentration, 500 mL subsamples in triplicate were filtered onto GF/F membrane (Whatman) under a low vacuum and stored in liquid nitrogen. The GF/F filters were then soaked into 5 mL of 90% acetone at 4°C in darkness for 20 h, centrifuged (4000 rpm for 10 min), and the suspensions were measured using Turner Design 7200 fluorometer with a nonacidification module (Welschmeyer 1994). The relative fluorescence units (RFU) were then converted to the Chl *a* concentration by multiplying a coefficient (*c*) that was derived from a calibration curve prepared by the relationship of a standard commercial Chl *a* from Sigma-Aldrich (C5753) with their corresponding RFU (Designs 2006; Li et al. 2021). The equation was Chl *a* concentration = $c \times$ RFU $\times$ extracted volume/filtered volume. To estimate the abundance of *Pseudo-nitzschia* and *Leptocylindrus*, at the beginning of the experiment and the end of each bottle, 100 mL seawater samples in triplicate was collected, fixed with 2% Lugol's solution (final concentration), and stored at room temperature. Diatoms were observed under the inverted microscopy at ×200 magnification (Olympus IX51) after 24 h of settlement. To minimize counting error, we randomly selected more than 30 views under the microscope to make sure over 500 target cells were enumerated for each diatom in each sample.

Growth rates and thermal traits estimate

The growth rates of *Pseudo-nitzschia* and *Leptocylindrus* were estimated following Landry et al. (2011). The net growth rate k (d^{-1}) was calculated as $k = 1/t \ln (A_i/(A_0 \times d_i))$, where A_0 is the cell abundance of diatoms at the beginning of incubation, A_i is the final cell abundance of diatoms of ith bottle after 1-d incubation, d_i is the dilution level (i.e., 10% or 100%), and t is the incubation time (1 d). As the grazing rate in the highly diluted bottles (10%) was negligible, $k_{10\%}$ equals the instantaneous growth rates under this scenario, that is, $k_{10\%} = \mu$ (Chen 2015; Morison and Menden-Deuer 2017; Anderson et al. 2022). For Stas. EP03 and P03, as no 10% dilution was setted for nutrient-unamended condition, growth rates in that case were estimated by $\mu_0 = k_{0100\%} + m$, where $k_{0100\%}$ is the net growth rate of diatoms in 100% dilution bottles under nutrient-unamended condition; m is the microzooplankton grazing rates, which according to the assumption of dilution approach should not be affected by the ambient nutrient conditions that could be calculated by $k_{n100\%} = \mu - m$, where $k_{n100\%}$ represents the net growth rates of diatoms in 100% dilution bottles in nutrient-amended treatment; μ equals $k_{n10\%}$ representing instantaneous growth under nutrient-amended conditions.

For the thermal performance curve drawing, the BA model can be used to predict thermal responses of metabolism-linked rates within the physiological temperature range (Gillooly et al. 2001; Pawar et al. 2016), where the rates show exponential increases with temperature. However, over a wide temperature regime, the thermal performance of metabolism-linked rates is usually unimodal, which can be described by the unimodal extension of the BA model (Johnson and Lewin 1946; Dell et al. 2011; Chen and Laws 2017) and expressed as

$$\mu = \mu_c \frac{e^{\frac{E_a}{K_b}\left(\frac{1}{T_c} - \frac{1}{T}\right)}}{1 + \frac{E_a}{E_h - E_a} e^{\frac{E_a}{K_b}\left(\frac{1}{T_{opt}} - \frac{1}{T}\right)}}, \quad (1)$$

where μ is the growth rate, E_a is the activation energy (eV) indicating temperature sensitivity, T is the absolute experimental temperature (K), T_c is the reference temperature, which was 288.15 K in this study, T_{opt} is the optimal temperature at which diatoms achieve the maximum growth rate (μ_{max}), E_h is the nominal activation energy that defines the effect of high-temperature inactivation when T exceeds T_{opt} (Chen 2022), μ_c is a normalization constant, and K_b is the Boltzmann constant (8.62×10^{-5} eV K^{-1}). T_{opt} and μ_{max} under each nutrient condition were derived from Eq. 1 implemented by the function *nls* in R (version 4.2.2) package *minpack.lm*. For the nutrient concentration (i.e., in situ nutrient condition at Stas. PM6 and PM7) that we cannot draw a nonlinear regression of the growth rates via Eq. 1 due to many negative values, we empirically identified T_{opt} as the experimental temperature where diatom achieved its highest experimental growth rates. All the values of T_{opt} and μ_{max}, as well as other parameters, are shown in the Supporting Information Tables S2 and S3.

Estimation of the effect of nutrient availability on T_{opt} and μ_{max}

We used the smooth term $s()$ in the generalized additive models (GAM) to describe the nonlinear effects of nutrient concentration in terms of DIN on T_{opt} and μ_{max} of *Pseudo-nitzschia* and *Leptocylindrus*. The GAM model is expressed as

$$T_{opt} \text{ or } \mu_{max} \sim s(\text{DIN}, \text{bs} = \text{"cs"}), \quad (2)$$

where T_{opt} and μ_{max} are derived from in situ manipulation experiments under different nutrient conditions (Supporting Information Tables S2, S3). DIN represents the concentration of in situ DIN plus the added DIN under each nutrient condition. The reason we chose DIN concentration as the nutrient availability representative is because of the limitation of DIN

19395590, 0, Downloaded from https://aslopubs.onlinelibrary.wiley.com/doi/10.1002/lno.12671 by University Of Strathclyde, Wiley Online Library on [02/09/2024]. See the Terms and Conditions (https://onlinelibrary.wiley.com/terms-and-conditions) on Wiley Online Library for rules of use; OA articles are governed by the applicable Creative Commons License

at our experimental stations (i.e., in situ DIN to dissolved inorganic phosphate [DIP] ratio < 16 : 1, except for Sta. EP03 (~ 23 : 1); Table 1). bs = "cs" represents the shrinkage version of cubic regression splines in the smooth function of GAM. GAM was implemented using the function *gam* in the R package "mgcv" (Wood 2017).

Long-term field data analyses

To further verify the effects of nutrient availability on natural diatom thermal response, we compiled and analyzed a 20-yr (from 2000 to 2020, except 2018) historical dataset of diatom abundances and corresponding environmental parameters measured at monthly intervals in Hong Kong coastal waters by the Environmental Protection Department of the Hong Kong SAR Government. The data were collected from the surface water (~0.5 m in depth) at three coastal stations, that is, WM2, WM3, and SM6 (Fig. 1), which are influenced by urbanized activities and the discharges from the Pearl River.

We used generalized additive mixed models (GAMMs; Wood 2017) to investigate the effects of nutrients and temperature on diatom cell abundances, with the consideration of random effects, that is, station. Besides the two focal genera, that is, *Pseudo-nitzschia* and *Leptocylindrus*, the cell abundance of total diatoms was also treated as the response variable to see whether the influence of nutrient availability on thermal response applies to the whole diatom assemblage. In our model, DIN and DIP concentration were both taken as potential descriptor variables together with temperature, for the reason of large variation of the DIN : DIP ratio during the long-term sampling period. Light, salinity, and silica concentration were also important factors influencing diatom growth and presence. For the light condition, as all the samples were collected from the surface layer and avoided extreme weather such as rain and heavy clouds, we think it may not be the limiting factor in our study. For salinity and silica concentration, they presented collinearity with DIN concentration, with either higher variance inflation factors (VIF > 3; Supporting Information Table S5; Zuur et al. 2009) or apparent correlation (Supporting Information Fig. S3). In addition, silica showed relatively high concentrations compared to DIN (Supporting Information Fig. S4), suggesting it might not be the limiting nutrient at the three stations. Hence, light, salinity, and silica concentration were not incorporated into the models.

We built several statistical models via GAMMs as mentioned above but narrowed down to two models based on their performances. One model treated temperature, DIN, and DIP as independent variables; another considered the interaction between temperature and DIN, for the reason that previous studies have revealed the high demands and uptake rates of nitrogen by diatoms (Litchman et al. 2007) and the important roles of nitrogen in regulating diatom cell density in other coastal regions (Xiao et al. 2018; Cheung et al. 2021). The statistical model without interaction between temperature and nutrients is given by

$$\log(Y) \sim s(\text{temperature}) + s(\text{DIN}) + s(\text{DIP}) + \alpha_s, \quad (3)$$

The model with the interaction of temperature and DIN is given by

$$\log(Y) \sim te(\text{temperature}, \text{DIN}) + s(\text{DIP}) + \alpha_s, \quad (4)$$

where Y is the response variable representing cell density of *Pseudo-nitzschia* and *Leptocylindrus* and total diatoms. Logarithmic transformation was used to normalize the asymmetrical frequency distribution of diatom cell density and nutrient concentrations. The term $s()$ indicates one-dimensional nonparametric smoothing function based on a cubic regression spline and $te()$ is a two-dimensional function of tensor product spline that shows the interactive effects of temperature and DIN. α_s represents the random effect, that is, station. Akaike's information criterion (AIC) and R^2 were examined to evaluate the performance of the statistical models. Overall, 709 total diatom observations, 489 *Pseudo-nitzschia* observations, and 261 *Leptocylindrus* observations, as well as their corresponding environmental factors, were put into each model. The GAMMs were performed using the *gamm* function in the *mcgv* package in R 4.2.2.

Results

Nutrients addition stimulate diatom growth at five experimental stations

Pseudo-nitzschia and *Leptocylindrus* accounted for 61.8–88.8% of in situ diatom cell abundance at the five manipulation experimental stations, with the genus *Leptocylindrus* mainly composed of *L. danicus* with a small proportion of *L. minimus* while the genus *Pseudo-nitzschia* mainly composed of *P. delicatissima* and *P. micropora* (Supporting Information Fig. S2). These two genera experienced high environmental temperatures and varying degrees of nutrient limitation (Table 1; Fig. 2). Adding nutrients at in situ temperature stimulated the growth of *Pseudo-nitzschia* and *Leptocylindrus* at all stations (Fig. 2a), indicating that these two diatom genera experienced nutrient limitation under ambient conditions. Under the conditions of highest nutrient enrichment, the mean growth rates among the five experimental stations were around three times higher than that under ambient nutrient concentrations (paired sample t-test, df = 4, $p = 0.025$ for *Pseudo-nitzschia*; $p < 0.001$ for *Leptocylindrus*; Fig. 2b).

Nutrients addition shift up the T_{opt} and μ_{max} of diatoms

At different nutrient addition levels, the growth rate of *Pseudo-nitzschia* and *Leptocylindrus* showed a unimodal pattern with temperature (Fig. 3). The T_{opt} of *Pseudo-nitzschia* and *Leptocylindrus* under in situ nutrient conditions was close to or lower than the in situ environmental temperature at the five

19395590, 0, Downloaded from https://aslopubs.onlinelibrary.wiley.com/doi/10.1002/lno.12671 by University Of Strathclyde, Wiley Online Library on [02/09/2024]. See the Terms and Conditions (https://onlinelibrary.wiley.com/terms-and-conditions) on Wiley Online Library for rules of use; OA articles are governed by the applicable Creative Commons License

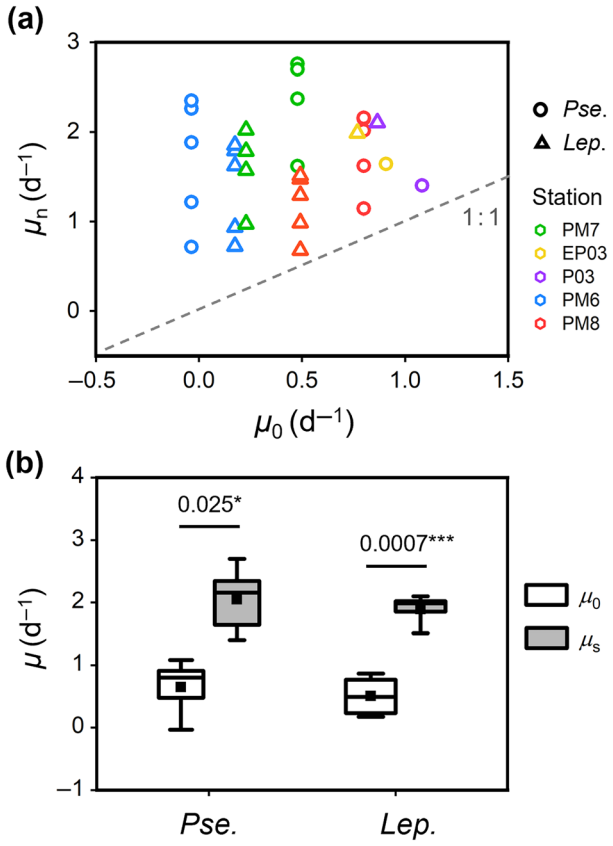

Fig. 2. Growth rates of *Pseudo-nitzschia* (*Pse.*) and *Leptocylindrus* (*Lep.*) at in situ temperature at five manipulation experimental stations. (**a**) Comparison of the growth rates under in situ nutrient conditions (μ_0) and nutrient-amended conditions (μ_n) at in situ temperature. Circles represent *Pse.* and triangles represent *Lep.* Different colors represent different stations. Each symbol represents the mean value of the growth rate estimated from duplicate bottles. (**b**) Growth rates of *Pse.* and *Lep.* under in situ nutrient condition (μ_0) and the highest nutrient addition level (μ_s) among the experimental stations ($n = 5$ for each box). The dashed line is the 1 : 1 line. *p*-value exhibits the significance level between μ_0 and μ_s (paired *t*-test: *$p < 0.05$; **$p < 0.01$; ***$p < 0.001$, $\alpha = 0.05$, df = 4).

experimental stations, except for *Pseudo-nitzschia* at Sta. EP03, where the in situ nutrient concentration was relatively high (Fig. 4a; Table 1). Increasing nutrient concentrations shifted the thermal curves of both *Pseudo-nitzschia* and *Leptocylindrus* up, changing the position of the curve's peak (Fig. 3). As such, the T_{opt} and μ_{max} of these two diatom genera increased with nutrient concentrations (Fig. 4a,b). The mean (± SD; $n = 5$) T_{opt} of *Pseudo-nitzschia* among the five experimental stations was 28.07 ± 1.62°C, which increased to 29.40 ± 0.72°C when adding the highest concentration of nutrients. Similarly, the T_{opt} of *Leptocylindrus* significantly increased from 27.25 ± 0.98°C to 29.72 ± 0.75°C (paired sample *t*-test, $p = 0.021$; df = 4; Fig. 4c). Simultaneously, the mean (± SD; $n = 5$) μ_{max} raised from 0.774 ± 0.297 d^{-1} under in situ nutrient condition to 2.088 ± 0.591 d^{-1} under the highest nutrient addition level for *Pseudo-nitzschia* (paired sample *t*-test, df = 4, $p = 0.028$ and from 0.607 ± 0.317 to 2.014 ± 0.307 d^{-1} for *Leptocylindrus* (paired sample *t*-test, df = 4, $p < 0.01$; Fig. 4d). Results of GAM showed significant effects of nutrient concentration on T_{opt} and μ_{max} of these two diatom genera ($p < 0.001$; Supporting Information Table S4), exhibiting saturation-like trends with increasing nutrient concentration (Fig. 4e,f).

Interaction effects of nutrient and temperature on diatoms based on long-term dataset

Analysis of the long-term dataset showed the seasonal and annual variations of total diatoms with a slightly increasing trend; also, the environmental factors including temperature, DIN, and DIP varied seasonally and annually (Fig. 5; Supporting Information Table S6). Comparing different GAMMs with various factor combinations, we found that the model with interactive effects of temperature and DIN concentration had higher R^2 and lower AIC than models excluding interaction effects (Supporting Information Table S7). In addition, the effects of these interaction terms on the cell density of *Pseudo-nitzschia*, *Leptocylindrus*, and total diatoms were significant ($p < 0.05$; Supporting Information Table S8), suggesting the interaction between temperature and DIN concentration can well explain the variations of diatom abundance. Based on the selected GAMMs, the high abundances of *Pseudo-nitzschia*, *Leptocylindrus*, and total diatoms were predicted under the conditions of high temperature and high DIN concentration (Fig. 6). Under high DIN concentration, rising temperature increased the abundance of diatoms. By contrast, under low DIN concentration, the abundance of *Pseudo-nitzschia* did not increase with increasing temperature, and the abundance of *Leptocylindrus* and total diatoms slightly decreased with rising temperature (Fig. 6). This result was consistent with the positive effect of nutrients on T_{opt} observed in our manipulation experiments.

Discussion

Temperature and nutrients are two primary factors affecting phytoplankton growth and biomass. We have extended the finding obtained from lab experiments (Thomas et al. 2017) to field diatom assemblages that nutrient limitation not only constrained growth rates of marine diatoms but also suppressed their T_{opt} and μ_{max}, which may lead to low abundances. Nutrient supply enabled marine diatoms to achieve better growth performance (i.e., higher μ_{max}) at the warmer environmental conditions (i.e., higher T_{opt}), suggesting the enhanced capacity against ocean warming under nutrient-abundant conditions.

Effects of nutrient availability on the thermal performance of *Pseudo-nitzschia* and *Leptocylindrus* in subtropical waters

Our study investigated the thermal performance of natural diatom genera in subtropical waters, where the ambient temperature is relatively high and may be experiencing rapid warming (Wu et al. 2012). Although the short-term temperature modulation experiments we performed strongly limited

19395590, 0, Downloaded from https://aslopubs.onlinelibrary.wiley.com/doi/10.1002/lno.12671 by University Of Strathclyde, Wiley Online Library on [02/09/2024]. See the Terms and Conditions (https://onlinelibrary.wiley.com/terms-and-conditions) on Wiley Online Library for rules of use; OA articles are governed by the applicable Creative Commons License

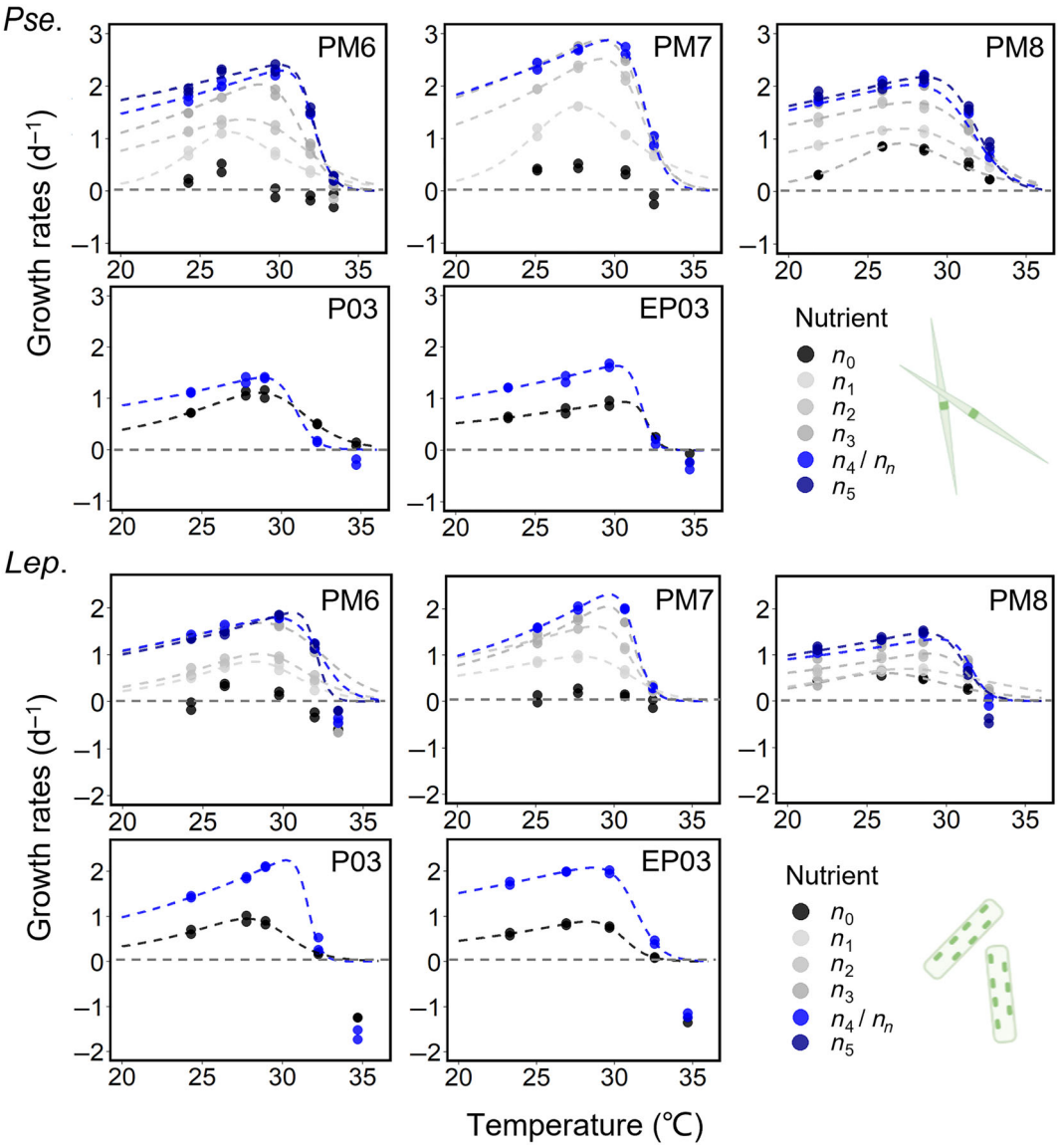

Fig. 3. Growth rates of *Pseudo-nitzschia* (*Pse.*) and *Leptocylindrus* (*Lep.*) in different nutrient addition levels at the experimental temperature regime at five manipulation stations. The color of dots indicates nutrient addition levels (n_0 is the in situ nutrient condition; n_1, n_2, n_3, n_4, and n_5 are different nutrient-amended levels at Stas. PM6, PM7, and PM8; n_n indicates nutrient-amended condition at Stas. EP03 and P03). The dashed curves are derived from the extended Boltzmann–Arrhenius model, with different colors representing corresponding nutrient addition levels.

our capacity to evaluate the future warming impacts over a long period, they still offered a valuable step to demonstrate the possible changes in the warming ocean. Our results showed that the current environmental temperature might be already beyond the physiological temperature range of *Pseudo-nitzschia* and *Leptocylindrus* growth, as the in situ environmental temperatures at most stations were close to or higher than their T_{opt} under the in situ nutrient condition (Fig. 4a). This is consistent with the previous research (Thomas et al. 2012), suggesting that (sub)tropical phytoplankton might be experiencing supra-optimal temperature from their ambient environments. Under this scenario, further warming would reduce the growth rates of *Pseudo-nitzschia* and *Leptocylindrus* in subtropical nutrient-limited waters. The response of biomass production might be similar, but needs further exploration as the two processes are not always coupled.

Increasing nutrient supply could enhance the thermal optima and maximum growth rates of *Pseudo-nitzschia* and *Leptocylindrus*. Nutrient availability is the key environmental factor influencing diatom global distribution and growth (McNair et al. 2018; Tréguer et al. 2018). In this study, we found nutrient limitation at all the experimental stations in summer, which aligns with previous observations in this area (Xia et al. 2015; Xu et al. 2022). The limited nutrients not

19395590, 0, Downloaded from https://aslopubs.onlinelibrary.wiley.com/doi/10.1002/lno.12671 by University Of Strathclyde, Wiley Online Library on [02/09/2024]. See the Terms and Conditions (https://onlinelibrary.wiley.com/terms-and-conditions) on Wiley Online Library for rules of use; OA articles are governed by the applicable Creative Commons License

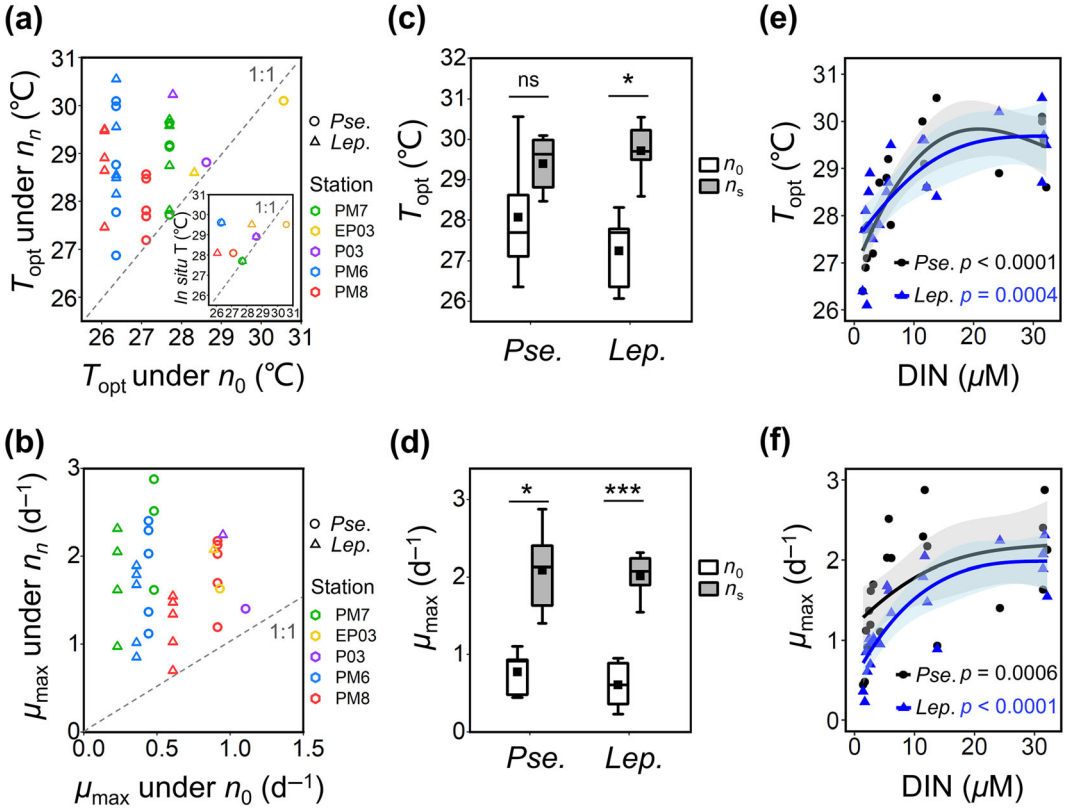

Fig. 4. Effects of nutrient concentration on the optimal growth temperature (T_{opt}) and maximum growth rate (μ_{max}) of *Pseudo-nitzschia* (*Pse.*) and *Leptocylindrus* (*Lep.*). Comparison of (**a**) T_{opt} and (**b**) μ_{max} under in situ nutrient conditions (n_0) and nutrient-amended conditions (n_n). The value of each symbol is derived from the extended Boltzmann–Arrhenius model under a specific nutrient concentration. Circles represent *Pse.* and triangles represent *Lep.* Different colors represent different stations. Comparison of the in situ environmental temperature (T) with the corresponding T_{opt} of these two diatom genera under n_0 at the five experimental stations is provided as an inner graph. The dashed lines are the 1 : 1 lines. (**c**) T_{opt} and (**d**) μ_{max} under n_0 and the highest nutrient addition level (n_s) among the five experimental stations ($n = 5$ for each box). *p*-value in (**c**) and (**d**) shows the significant values by paired sample *t*-test (*$p < 0.05$; **$p < 0.01$; ***$p < 0.001$; ns, no significant difference; df = 4). Effects of nutrient concentration in terms of dissolved inorganic nitrogen (DIN) on (**e**) T_{opt} and (**f**) μ_{max}. Data are fitted with a cubic spline smooth function in the generalized additive models. Black dots and lines represent *Pse.* and blue triangles and lines represent *Lep.* The shaded area in (**e**) and (**f**) represents 95% confidence intervals; *p*-value indicates the significance of the nutrient effects ($n = 21$).

only reduced growth rates of *Pseudo-nitzschia* and *Leptocylindrus* but also their T_{opt} and μ_{max} (Figs. 2, 4). Adding nutrients raised T_{opt} of both diatom genera, with the phenomenon more pronounced at three PM stations due to the extremely low in situ nutrient concentrations (Fig. 4; Table 1). Our findings are consistent with the previous laboratory study on *T. pseudonana* (Thomas et al. 2017), suggesting that T_{opt} is a saturating function of nutrient concentration. Another in situ manipulated experiment, although not comparing T_{opt} directly, also found that natural phytoplankton was less tolerant to high temperatures when there was insufficient nutrient supply (Anderson et al. 2022). Simultaneously, μ_{max} showed a similar response to nutrient availability as T_{opt}, which, together, demonstrated that higher nutrient availability could not only improve the thermal optima of *Pseudo-nitzschia* and *Leptocylindrus* but also favor them to flourish under the warming ocean.

The underlying mechanism of nutrient limitation suppressing μ_{max} of natural diatom is probably the constrained enzymatic kinetics caused by fewer substrates/resources, which has been well studied in terrestrial ecology (Davidson and Janssens 2006; German et al. 2012). Briefly, increasing temperature within the physiological temperature range leads to higher substrate kinetic energy, collision rate, and structural flexibility of enzymes, which ultimately promotes catalytic rates (Somero 1995, 2004; Marañón et al. 2014). However, when there is low nutrient concentration, which offers fewer substrates/resources for phytoplankton growth, the capability of nutrient uptake kinetics will be constrained. The restricted substrates/resources may not support the high applicability of enzymatic kinetics at higher temperatures, hence suppressing μ_{max}. Also, under nutrient-limited conditions, T_{opt} was reduced in concert with μ_{max}. As the limited nutrient restricted the further increase of growth rate as temperature increases, the peak of the thermal curve was achieved at a lower temperature. Another possible explanation is that the half-saturation constant (K_n, indicating the nutrient concentration

19395590, 0, Downloaded from https://aslopubs.onlinelibrary.wiley.com/doi/10.1002/lno.12671 by University Of Strathclyde, Wiley Online Library on [02/09/2024]. See the Terms and Conditions (https://onlinelibrary.wiley.com/terms-and-conditions) on Wiley Online Library for rules of use; OA articles are governed by the applicable Creative Commons License

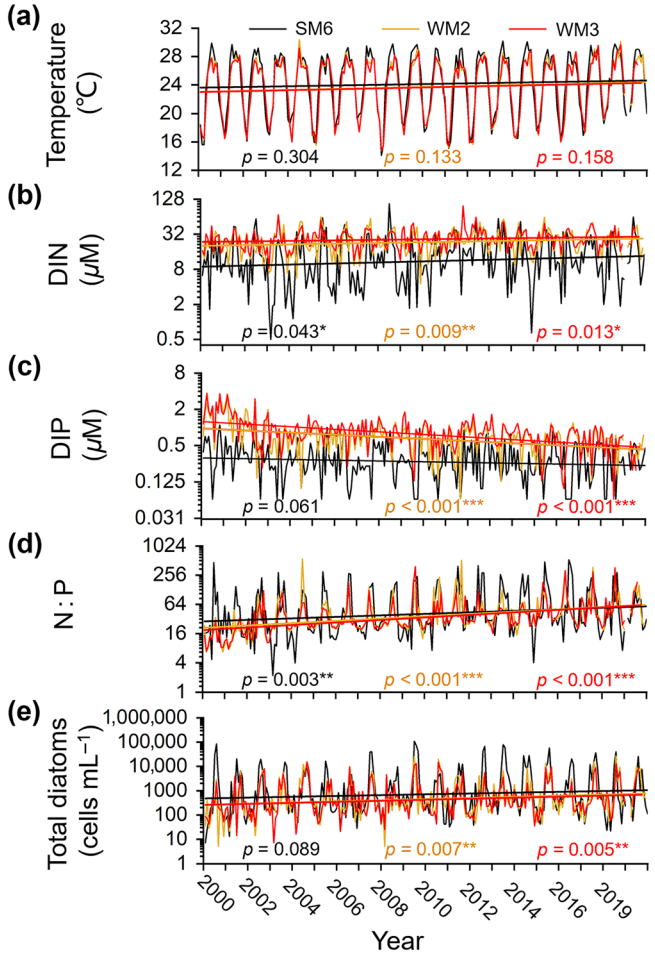

Fig. 5. Long-term variation of temperature, nutrient concentration, and total diatom cell density in three monitoring stations. (**a**) Temperature. (**b**) Concentration of dissolved inorganic nitrogen (DIN) and (**c**) phosphate (DIP). (**d**) Ratio of DIN to DIP concentration (N : P). (**e**) Cell density of total diatoms. Black, yellow, and red colors represent Stas. SM6, WM2, and WM3, respectively. Trend lines are produced via linear regression, with the *p*-value representing significant values (*$p < 0.05$; **$p < 0.01$; ***$p < 0.001$).

that phytoplankton achieves half-maximum nutrient uptake rates or growth rates) increases with rising temperature, suggesting a decrease in enzyme kinetic efficiency and, possibly, enzyme affinity (Bestion et al. 2018; Liu et al. 2021). Therefore, we observed low T_{opt} values under the nutrient-limited conditions.

Environmental nutrient availability affects marine diatoms coping with higher temperatures: Evidence from a 20-yr historical dataset analysis

In addition to estimating the short-term growth rate and thermal response of natural diatom genera, we further examined the long-term variations of diatom abundance in varying temperature and nutrient conditions. The analysis of a 20-yr historical dataset in Hong Kong coastal waters supports our findings in manipulation experiments, indicating that environmental nutrient availability affects diatoms (in terms of cell density) coping with higher temperatures. Using in situ growth data to investigate the thermal performance of marine plankton over a large geographical or temporal scale is impractical due to the limitation of manpower and experimental conditions. As such, some studies used cell abundance to substitute growth rate to investigate plankton thermal response (Burrows et al. 2019), even though the results might have some discrepancies, as the cell abundance could be influenced by multiple factors in nature and more closely resembles a proxy for net growth rates rather than intrinsic growth rates. Diatoms have been identified as the fast-growing "opportunist" in natural environments (Dutkiewicz et al. 2009; Ward et al. 2012; McNair et al. 2018). In contrast with other phytoplankton, such as coccolithophorids and dinoflagellates, the typical *r*-strategy drives diatom fast division, high growth rates, and rapid responses in facing fluctuating environments (Kilham and Hecky 1988; Dutkiewicz et al. 2009). Therefore, the high cell density of diatoms in changing environments is usually accompanied by their higher growth rates, with their predators performing a notable time lag (Tréguer et al. 2018).

In this part, we found that, under DIN-limited conditions, higher temperatures either showed marginal impacts (i.e., on *Pseudo-nitzschia*) or apparently inhibited cell density of marine diatoms (i.e., *Leptocylindrus* and total diatoms; Fig. 6). In contrast, higher temperatures favored the proliferation of natural diatoms when there was enough DIN supply (Fig. 6). Together, it is indicated that nutrient-rich environments enable marine diatoms to flourish at higher temperatures, which echoes our results from in situ manipulation experiments. Our findings of temperature–nutrient interplay influencing natural diatom dynamics agree with the previous research in the estuarine ecosystems (Xiao et al. 2018; Cheung et al. 2021). One study in the East China Sea suggested that diatoms could better tolerate high temperatures under relatively high nitrate concentrations, whereas their intolerance to high temperatures is attributed to the additional stress of nutrient limitation rather than their inherent metabolic response (Xiao et al. 2018). Another study in the PRE also found that warming and high nitrate concentration additively promoted diatom abundance (Cheung et al. 2021).

In addition, our research on the historical data, in line with the findings of Xiao et al. (2018) and Cheung et al. (2021), highlights the significant role of ambient DIN concentration on diatom cell density in coastal regions. One possible explanation could be the high nitrate utilizing efficiency of marine diatoms induced by high active nitrate reductase and more nitrate transporters and their large nitrate demands (Litchman et al. 2007; Glibert et al. 2016; Glibert 2020). On the other hand, when high temperatures and DIN loading favor diatoms in our study area, it is accompanied by a high N : P ratio and relatively low DIP concentration (Fig. 6). This could be the result of both the high N : P discharge by the Pearl River during the summer and the further depletion of DIP caused by the scavenging effect of diatoms.

19395590, 0, Downloaded from https://aslopubs.onlinelibrary.wiley.com/doi/10.1002/lno.12671 by University Of Strathclyde, Wiley Online Library on [02/09/2024]. See the Terms and Conditions (https://onlinelibrary.wiley.com/terms-and-conditions) on Wiley Online Library for rules of use; OA articles are governed by the applicable Creative Commons License

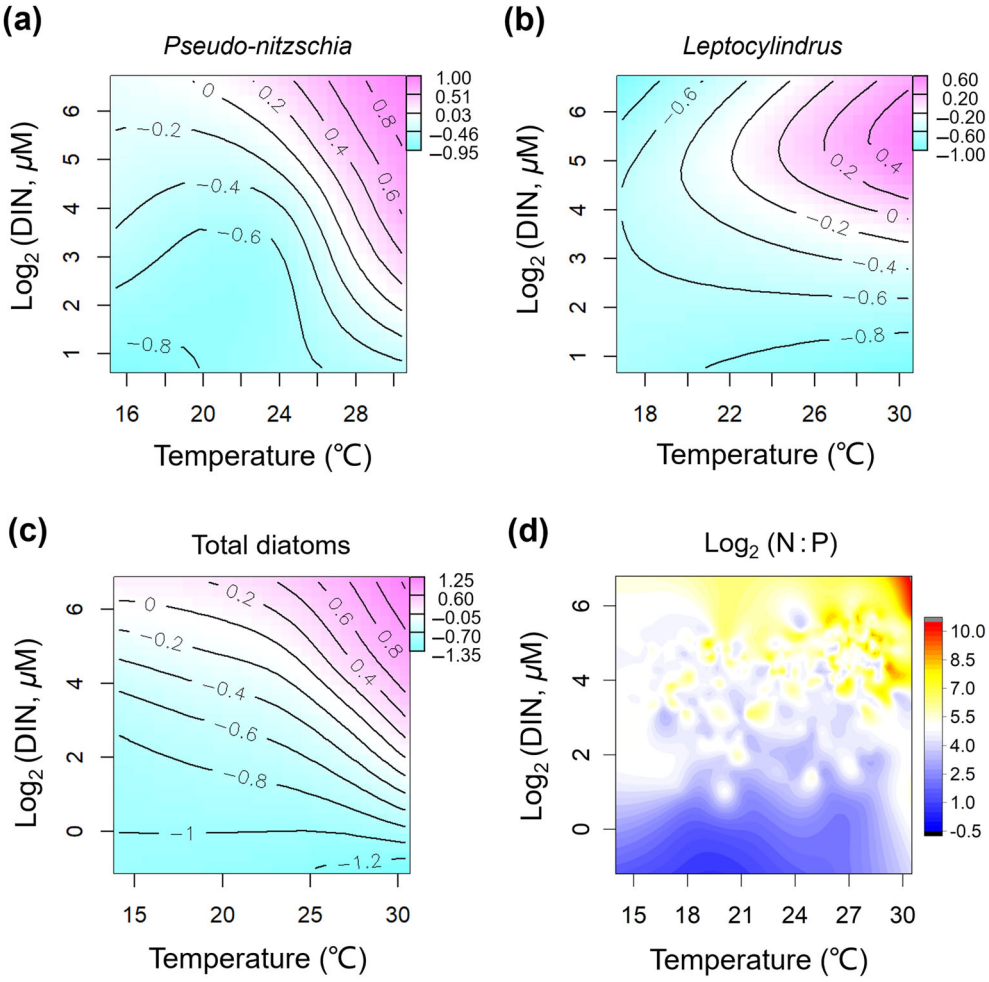

Fig. 6. The interactive effects of temperature and dissolved inorganic nitrogen (DIN) concentration on cell density of (**a**) *Pseudo-nitzschia*, (**b**) *Leptocylindrus*, and (**c**) total diatoms. The gradient color and line represent the partial interaction effects of DIN and temperature on relative diatom cell abundances. (**d**) The contour plot shows the N : P ratio varying with different DIN and temperature combinations, which is made by *Origin 2019* (OriginLab). DIN concentration and N : P are log-transformed.

Implications of nutrient availability influencing thermal response of marine diatoms under global warming

Effects of nutrients and temperature on phytoplankton in natural environments are never independent. The future sea surface temperature will increase by 1–4°C by the end of the 21st century (Edenhofer et al. 2013). Combining this warming scenario with the T_{opt} of *Pseudo-nitzschia* and *Leptocylindrus* in our investigated subtropical nutrient-limited manipulation stations (i.e., T_{opt} under in situ nutrient condition was close to or mostly higher than the current ambient temperature; Fig. 4a), diatoms in nutrient-insufficient (sub)tropical waters may face a perilous future, with the possible consequences being a decrease in biodiversity and primary production (Hooper et al. 2012; Thomas et al. 2012).

However, nutrient-rich environments can enhance marine diatoms to tolerate high temperatures and favor them to achieve higher growth rates and higher cell density in warmer conditions. Such kind of thermoplasticity may generate positive feedback after long-term warming adaptation under nutrient-sufficient conditions, resulting in further improvements to their T_{opt} and μ_{max} (Schaum et al. 2017; O'Donnell et al. 2018), whereas it might inhibit diatom adaptation to high temperature when nutrient-limited (Aranguren-Gassis et al. 2019). Our long-term observation found a marked increase in diatom cell density from 2000 to 2020, which might be ascribed to slight warming and significantly elevated DIN concentration (Fig. 5; Supporting Information Table S6). Total nitrogen concentration in the PRE has been increasing since the 1990s due to anthropogenic inputs such as the increased usage of fertilizers in agriculture (Huan et al. 2016; Xuan et al. 2020; Cheung et al. 2021). Considering the ongoing urbanization of the Greater Bay Area in China, nitrogen concentration is very likely to increase continuously at a fast pace (Dai et al. 2008; Xuan et al. 2020). In that case, warming may favor diatoms' proliferation in the

19395590, 0, Downloaded from https://aslopubs.onlinelibrary.wiley.com/doi/10.1002/lno.12671 by University Of Strathclyde, Wiley Online Library on [02/09/2024]. See the Terms and Conditions (https://onlinelibrary.wiley.com/terms-and-conditions) on Wiley Online Library for rules of use; OA articles are governed by the applicable Creative Commons License

subtropical nutrient-rich regions such as estuarine ecosystems. However, determining whether this proliferation will benefit these ecosystems (e.g., increasing primary production) or lead to potential negative consequences (e.g., hypoxia) necessitates further investigation and discussion.

Our study highlights the influence of nutrient availability on marine diatom thermal response in nature, with rising temperatures hampering the growth of diatoms in nutrient-limited waters while benefiting them in nutrient-rich environments. Here, we emphasize the significance of accounting for the joint effects of the environmental factors when predicting ecosystem response to climate warming. Since our assessments of diatom growth performance relied on the short-term dilution technique, future study is needed to study their adaptative behavior and mechanisms over a longer timescale to ascertain if the acute response aligns with the acclimated physiological response. Besides, it is also necessary to investigate the species-specific thermal response for marine diatoms and other phytoplankton groups.

Data availability statement

The data that support the findings of this study are openly available in the GitHub repository at https://github.com/pangmengwen/diatom-thermal-response.git.

References

Anderson, S. I., and others. 2022. The interactive effects of temperature and nutrients on a spring phytoplankton community. Limnol. Oceanogr. **67**: 634–645. doi:10.1002/lno.12023

Aranguren-Gassis, M., C. T. Kremer, C. A. Klausmeier, and E. Litchman. 2019. Nitrogen limitation inhibits marine diatom adaptation to high temperatures. Ecol. Lett. **22**: 1860–1869. doi:10.1111/ele.13378

Bestion, E., B. García-Carreras, C. E. Schaum, S. Pawar, and G. Yvon-Durocher. 2018. Metabolic traits predict the effects of warming on phytoplankton competition. Ecol. Lett. **21**: 655–664. doi:10.1111/ele.12932

Brown, J. H., J. F. Gillooly, A. P. Allen, V. M. Savage, and G. B. West. 2004. Toward a metabolic theory of ecology. Ecology **85**: 1771–1789. doi:10.1890/03-9000

Burrows, M. T., and others. 2019. Ocean community warming responses explained by thermal affinities and temperature gradients. Nat. Clim. Change **9**: 959–963.

Chen, B. 2015. Assessing the accuracy of the "two-point" dilution technique. Limnol. Oceanogr.: Methods **13**: 521–526. doi:10.1002/lom3.10044

Chen, B. 2022. Thermal diversity affects community responses to warming. Ecol. Model. **464**: 109846. doi:10.1016/j.ecolmodel.2021.109846

Chen, B., M. R. Landry, B. Huang, and H. Liu. 2012. Does warming enhance the effect of microzooplankton grazing on marine phytoplankton in the ocean? Limnol. Oceanogr. **57**: 519–526. doi:10.4319/lo.2012.57.2.0519

Chen, B., and E. A. Laws. 2017. Is there a difference of temperature sensitivity between marine phytoplankton and heterotrophs? Limnol. Oceanogr. **62**: 806–817. doi:10.1002/lno.10462

Cheung, Y. Y., S. Cheung, J. Mak, K. Liu, X. Xia, X. Zhang, Y. Yung, and H. Liu. 2021. Distinct interaction effects of warming and anthropogenic input on diatoms and dinoflagellates in an urbanized estuarine ecosystem. Glob. Chang. Biol. **27**: 3463–3473. doi:10.1111/gcb.15667

Collins, M., and others. 2013. Long-term climate change: Projections, commitments and irreversibility, p. 1029–1136. *In* T. F. Stocker and others [eds.], Climate change 2013: The physical science basis. Contribution of Working Group I to the fifth assessment report of the Intergovernmental Panel on Climate Change. Cambridge Univ. Press.

Dai, M., L. Wang, X. Guo, W. Zhai, Q. Li, B. He, and S. J. Kao. 2008. Nitrification and inorganic nitrogen distribution in a large perturbed river/estuarine system: The Pearl River Estuary, China. Biogeosciences **5**: 1227–1244. doi:10.5194/bg-5-1227-2008

Davidson, E. A., and I. A. Janssens. 2006. Temperature sensitivity of soil carbon decomposition and feedbacks to climate change. Nature **440**: 165–173.

Dell, A. I., S. Pawar, and V. M. Savage. 2011. Systematic variation in the temperature dependence of physiological and ecological traits. Proc. Natl. Acad. Sci. USA **108**: 10591–10596. doi:10.1073/pnas.1015178108

Dutkiewicz, S., M. J. Follows, and J. G. Bragg. 2009. Modeling the coupling of ocean ecology and biogeochemistry. Global Biogeochem. Cycles **23**: 1–15. doi:10.1029/2008GB003405

Edenhofer, O., K. Seyboth, and J. F. Shogren. 2013. Intergovernmental Panel on Climate Change (IPCC), p. 48–56. *In* Encyclopedia of energy, natural resource, and environmental economics, v. 1. Elsevier.

Elser, J. J., and others. 2007. Global analysis of nitrogen and phosphorus limitation of primary producers in freshwater, marine and terrestrial ecosystems. Ecol. Lett. **10**: 1135–1142. doi:10.1111/j.1461-0248.2007.01113.x

Eppley, R. W. 1972. Temperature and phytoplankton growth in the sea. Fish. Bull. **70**: 1063–1085.

Falkowski, P. 2012. Ocean science: The power of plankton. Nature **483**: 17–20. doi:10.1038/483S17a

Field, C. B., M. J. Behrenfeld, J. T. Randerson, and P. Falkowski. 1998. Primary production of the biosphere: Integrating terrestrial and oceanic components. Science **281**: 237–240. doi:10.1126/science.281.5374.237

Fussmann, K. E., F. Schwarzmüller, U. Brose, A. Jousset, and B. C. Rall. 2014. Ecological stability in response to warming. Nat. Clim. Change **4**: 206–210. doi:10.1038/nclimate2134

German, D. P., K. R. Marcelo, M. M. Stone, and S. D. Allison. 2012. The Michaelis–Menten kinetics of soil extracellular enzymes in response to temperature: A cross-latitudinal

19395590, 0, Downloaded from https://aslopubs.onlinelibrary.wiley.com/doi/10.1002/lno.12671 by University Of Strathclyde, Wiley Online Library on [02/09/2024]. See the Terms and Conditions (https://onlinelibrary.wiley.com/terms-and-conditions) on Wiley Online Library for rules of use; OA articles are governed by the applicable Creative Commons License

study. Glob. Chang. Biol. **18**: 1468–1479. doi:10.1111/j.1365-2486.2011.02615.x

Gillooly, J. F., J. H. Brown, G. B. West, V. M. Savage, and E. L. Charnov. 2001. Effects of size and temperature on metabolic rate. Science **293**: 2248–2251. doi:10.1126/science.1061967

Glibert, P. M. 2020. Harmful algae at the complex nexus of eutrophication and climate change. Harmful Algae **91**: 101583. doi:10.1016/j.hal.2019.03.001

Glibert, P. M., and others. 2016. Pluses and minuses of ammonium and nitrate uptake and assimilation by phytoplankton and implications for productivity and community composition, with emphasis on nitrogen-enriched conditions. Limnol. Oceanogr. **61**: 165–197. doi:10.1002/lno.10203

Hooper, D. U., and others. 2012. A global synthesis reveals biodiversity loss as a major driver of ecosystem change. Nature **486**: 105–108. doi:10.1038/nature11118

Huan, Q. L., R. S. Pang, Q. L. Zhou, and K. M. Leng. 2016. Variation trends of nitrogen and phosphorus and the relationship with HABs in Shenzhen coastal waters. Mar. Environ. Sci. **35**: 908–914. doi:10.13634/j.cnki.mes20160617

Irwin, A. J., and M. J. Oliver. 2009. Are ocean deserts getting larger? Geophys. Res. Lett. **36**: 1–5. doi:10.1029/2009GL039883

Johnson, F. H., and I. Lewin. 1946. The growth rate of *E. coli* in relation to temperature, quinine and coenzyme. J. Cell. Comp. Physiol. **28**: 47–75. doi:10.1002/jcp.1030280104

Kilham, P., and R. E. Hecky. 1988. Comparative ecology of marine and freshwater phytoplankton 1. Limnol. Oceanogr. **33**: 776–795. doi:10.4319/lo.1988.33.4part2.0776

Knap, A. H., A. Michaels, A. R. Close, H. Ducklow, and A. G. Dickson. 1994. Protocols for the joint global ocean flux study (JGOFS) core measurements. JGOFS Report No. 19. Reprint of the IOC Manuals and Guides No. 29, UNESCO.

Landry, M. R., and R. P. L. Hassett. 1982. Estimating the grazing impact of marine micro-zooplankton. Mar. Biol. **67**: 283–288. doi:10.1007/BF00397668

Landry, M. R., K. E. Selph, and E. J. Yang. 2011. Decoupled phytoplankton growth and microzooplankton grazing in the deep euphotic zone of the eastern equatorial Pacific. Mar. Ecol. Prog. Ser. **421**: 13–24. doi:10.3354/meps08792

Lehtinen, S., T. Tamminen, R. Ptacnik, and T. Andersen. 2017. Phytoplankton species richness, evenness, and production in relation to nutrient availability and imbalance. Limnol. Oceanogr. **62**: 1393–1408. doi:10.1002/lno.10506

Li, W., J. Ge, P. Ding, J. Ma, P. M. Glibert, and D. Liu. 2021. Effects of dual fronts on the spatial pattern of chlorophyll-a concentrations in and off the Changjiang River Estuary. Estuar. Coasts **44**: 1408–1418. doi:10.1007/s12237-020-00893-z

Litchman, E., C. A. Klausmeier, O. M. Schofield, and P. G. Falkowski. 2007. The role of functional traits and trade-offs in structuring phytoplankton communities: Scaling from cellular to ecosystem level. Ecol. Lett. **10**: 1170–1181. doi:10.1111/j.1461-0248.2007.01117.x

Liu, K., B. Chen, S. Zhang, M. Sato, Z. Shi, and H. Liu. 2019. Marine phytoplankton in subtropical coastal waters showing lower thermal sensitivity than microzooplankton. Limnol. Oceanogr. **64**: 1103–1119. doi:10.1002/lno.11101

Liu, K., K. Suzuki, B. Chen, and H. Liu. 2021. Are temperature sensitivities of *Prochlorococcus* and *Synechococcus* impacted by nutrient availability in the subtropical northwest Pacific? Limnol. Oceanogr. **66**: 639–651. doi:10.1002/lno.11629

Malviya, S., and others. 2016. Insights into global diatom distribution and diversity in the world's ocean. Proc. Natl. Acad. Sci. USA **113**: 1516–1525. doi:10.1073/pnas.1509523113

Marañón, E., P. Cermeño, M. Huete-Ortega, D. C. López-Sandoval, B. Mouriño-Carballido, and T. Rodríguez-Ramos. 2014. Resource supply overrides temperature as a controlling factor of marine phytoplankton growth. PLoS One **9**: 1–8. doi:10.1371/journal.pone.0099312

Marañón, E., P. Cermeno, M. Latasa, and R. D. Tadonléké. 2015. Resource supply alone explains the variability of marine phytoplankton size structure. Limnol. Oceanogr. **60**: 1848–1854. doi:10.1002/lno.10138

McNair, H. M., M. A. Brzezinski, and J. W. Krause. 2018. Diatom populations in an upwelling environment decrease silica content to avoid growth limitation. Environ. Microbiol. **20**: 4184–4193. doi:10.1111/1462-2920.14431

Moore, C. M., and others. 2013. Processes and patterns of oceanic nutrient limitation. Nat. Geosci. **6**: 701–710. doi:10.1016/j.ecss.2007.05.014

Morison, F., and S. Menden-Deuer. 2017. Doing more with less? Balancing sampling resolution and effort in measurements of protistan growth and grazing-rates. Limnol. Oceanogr.: Methods **15**: 794–809. doi:10.1002/lom3.10200

Nelson, D. M., P. Tréguer, M. A. Brzezinski, A. Leynaert, and B. Quéguiner. 1995. Production and dissolution of biogenic silica in the ocean: Revised global estimates, comparison with regional data and relationship to biogenic sedimentation. Global Biogeochem. Cycles **9**: 359–372. doi:10.1029/95GB01070

O'Connor, M. I., M. F. Piehler, D. M. Leech, A. Anton, and J. F. Bruno. 2009. Warming and resource availability shift food web structure and metabolism. PLoS Biol. **7**: e1000178. doi:10.1371/journal.pbio.1000178

O'Donnell, D. R., C. R. Hamman, E. C. Johnson, C. T. Kremer, C. A. Klausmeier, and E. Litchman. 2018. Rapid thermal adaptation in a marine diatom reveals constraints and trade-offs. Glob. Chang. Biol. **24**: 4554–4565. doi:10.1111/gcb.14360

Pawar, S., A. I. Dell, V. M. Savage, and J. L. Knies. 2016. Real versus artificial variation in the thermal sensitivity of biological traits. Am. Nat. **187**: E41–E52. doi:10.1086/684590

Polovina, J. J., E. A. Howell, and M. Abecassis. 2008. Ocean's least productive waters are expanding. Geophys. Res. Lett. **35**: 1–5. doi:10.1029/2007GL031745

19395590, 0, Downloaded from https://aslopubs.onlinelibrary.wiley.com/doi/10.1002/lno.12671 by University Of Strathclyde, Wiley Online Library on [02/09/2024]. See the Terms and Conditions (https://onlinelibrary.wiley.com/terms-and-conditions) on Wiley Online Library for rules of use; OA articles are governed by the applicable Creative Commons License

Sarmiento, J. L., and others. 2004. Response of ocean ecosystems to climate warming. Global Biogeochem. Cycles **18**: 1–23. doi:10.1029/2003GB002134

Schaum, C. S., and others. 2017. Adaptation of phytoplankton to a decade of experimental warming linked to increased photosynthesis. Nat. Ecol. Evol. **1**: 1–7. doi:10.1038/s41559-017-0094

Somero, G. N. 1995. Proteins and temperature. Annu. Rev. Physiol. **57**: 43–68.

Somero, G. N. 2004. Adaptation of enzymes to temperature: Searching for basic "strategies". Comp. Biochem. Physiol. B Biochem. Mol. Biol. **139**: 321–333. doi:10.1016/j.cbpc.2004.05.003

Thomas, M. K., C. T. Kremer, C. A. Klausmeier, and E. Litchman. 2012. A global pattern of thermal adaptation in marine phytoplankton. Science **338**: 1085–1088. doi:10.1126/science.1224836

Thomas, M. K., M. Aranguren-Gassis, C. T. Kremer, M. R. Gould, K. Anderson, C. A. Klausmeier, and E. Litchman. 2017. Temperature–nutrient interactions exacerbate sensitivity to warming in phytoplankton. Glob. Chang. Biol. **23**: 3269–3280. doi:10.1111/gcb.13641

Tréguer, P., and others. 2018. Influence of diatom diversity on the ocean biological carbon pump. Nat. Geosci. **11**: 27–37. doi:10.1038/s41561-017-0028-x

Turner Designs. 2006. Trilogy laboratory fluorometer user's manual. Version 1. p. 38.

Ward, B. A., S. Dutkiewicz, O. Jahn, and M. J. Follows. 2012. A size-structured food-web model for the global ocean. Limnol. Oceanogr. **57**: 1877–1891. doi:10.4319/lo.2012.57.6.1877

Welschmeyer, N. A. 1994. Fluorometric analysis of chlorophyll a in the presence of chlorophyll b and pheopigments. Limnol. Oceanogr. **39**: 1985–1992. doi:10.4319/lo.1994.39.8.1985

Wood, S. N. 2017. Generalized additive models: An introduction with R. CRC Press.

Wu, L., and others. 2012. Enhanced warming over the global subtropical western boundary currents. Nat. Clim. Change **2**: 161–166. doi:10.1038/nclimate1353

Xia, X., N. K. Vidyarathna, B. Palenik, P. Lee, and H. Liu. 2015. Comparison of the seasonal variations of *Synechococcus* assemblage structures in estuarine waters and coastal waters of Hong Kong. Appl. Environ. Microbiol. **81**: 7644–7655. doi:10.1128/AEM.01895-15

Xiao, W., X. Liu, A. J. Irwin, E. A. Laws, L. Wang, B. Chen, Y. Zeng, and B. Huang. 2018. Warming and eutrophication combine to restructure diatoms and dinoflagellates. Water Res. **128**: 206–216. doi:10.1016/j.watres.2017.10.051

Xu, M. N., and others. 2022. Diel change in inorganic nitrogenous nutrient dynamics and associated oxygen stoichiometry along the Pearl River Estuary. Water Res. **222**: 118954. doi:10.1016/j.watres.2022.118954

Xuan, Y., C. Tang, and Y. Cao. 2020. Mechanisms of nitrate accumulation in highly urbanized rivers: Evidence from multi-isotopes in the Pearl River Delta, China. J. Hydrol. **587**: 124924. doi:10.1016/j.jhydrol.2020.124924

Zuur, A. F., E. N. Ieno, N. J. Walker, A. A. Saveliev, and G. M. Smith. 2009. Mixed effects models and extensions in ecology with R, v. **574**. Springer. doi:10.1007/978-0-387-87458-6

Acknowledgments

We sincerely thank Miss. Huijun Wu, Mr. Cheng Qian, and Dr. Weiguo Zhou for the sample collection, the Environmental Protection Department of the Hong Kong SAR Government for the historical data, Yanjiao Lai for the nutrient measurements, and Hongxing Cui for the recommendation on data analysis. This research was supported by the National Key Research and Development Program of China (2022YFC3105301), the National Science Foundation of China (42306103), and the Environmental Research, Technology Demonstration, and Conference Projects (ECF 2021-2119) from the Environment and Conservation Fund of the Hong Kong SAR government.

Conflict of Interest

None declared.

Submitted 22 May 2023
Revised 20 January 2024
Accepted 10 August 2024

Associate editor: Tatiana Rynearson

19395590, 0, Downloaded from https://aslopubs.onlinelibrary.wiley.com/doi/10.1002/lno.12671 by University Of Strathclyde, Wiley Online Library on [02/09/2024]. See the Terms and Conditions (https://onlinelibrary.wiley.com/terms-and-conditions) on Wiley Online Library for rules of use; OA articles are governed by the applicable Creative Commons License